Title
Pronghorn: Porous media thermal-hydraulics for reactor applications

Authors
Novak, AJ
Zou, L
Peterson, JW
et al.

Publication Date
2018

Peer reviewed

Pronghorn: Porous Media Thermal-Hydraulics for Reactor Applications

April J. Novak,* Ling Zou,† John W. Peterson,† Richard C. Martineau,† and Rachel N. Slaybaugh*

*University of California-Berkeley, Berkeley, CA {novak, slaybaugh}@berkeley.edu
†Idaho National Laboratory, P.O. Box 1625, Idaho Falls, ID {ling.zou, jw.peterson, richard.martineau}@inl.gov

INTRODUCTION

Pebble bed High Temperature Reactors (HTRs) are characterized by many advantageous design features, such as excellent passive heat removal in accidents and large margins to fuel failure. However, a significant challenge in thermal-hydraulic core modeling of pebble bed reactors is the double heterogeneity random packing of hundreds of thousands of fuel pebbles and thousands of fuel particles per pebble. A new porous media thermal-hydraulics code, Pronghorn, is under development to provide a fast-running, medium-fidelity core simulator and serve as a bridge between low-resolution system level codes and high-resolution Computational Fluid Dynamics (CFD) codes for multiscale analysis. Pronghorn is based on the Multiphysics Object-Oriented Simulation Environment (MOOSE) finite element framework, and permits an arbitrary equation of state, unstructured mesh capabilities, modern software design, and the ability to couple to MOOSE fuels performance and systems-level Thermal-Hydraulic (T/H) codes. To address the wide variety in gas- and liquid-cooled pebble bed reactor designs, Pronghorn includes several different flow models, each most appropriate to a range of compressibilities and operating conditions. This paper reviews benchmarking efforts of a low-advection flow model appropriate for Loss of Forced Circulation (LOFC) simulations and introduces the new fully compressible flow model with preliminary validation by comparison to potential flow theory for low Mach number flow over a cylinder.

THEORY

The porous media equations are obtained by averaging the Navier-Stokes equations in space over a heterogeneous mixture of fluid and solid phases. Assuming thermal non-equilibrium between the fluid and solid phases, this equation set includes conservation of fluid mass, momentum, and energy, coupled to conservation of the solid phase energy,

$$\frac{\partial(\epsilon\rho_f)}{\partial t} + \nabla\cdot(\epsilon\rho_f \boldsymbol{V}) = 0\,, \tag{1}$$

$$\frac{\partial(\epsilon\rho_f \boldsymbol{V})}{\partial t} + \nabla\cdot(\epsilon\rho_f \boldsymbol{V}\boldsymbol{V}) + \epsilon\nabla P - \epsilon\rho_f \boldsymbol{g} + W\rho_f \boldsymbol{V} = 0\,, \tag{2}$$

$$\frac{\partial(\epsilon\rho_f E_f)}{\partial t} + \nabla\cdot(\epsilon\rho_f H_f \boldsymbol{V}) - \epsilon\rho_f \boldsymbol{g}\cdot\boldsymbol{V} - \nabla\cdot(\epsilon k_f \nabla T_f) + \alpha(T_f - T_s) - \dot{q}_f = 0 \tag{3}$$

$$(1-\epsilon)\rho_s C_{p,s}\frac{\partial T_s}{\partial t} + (1-\epsilon)\rho_s C_{p,s}\boldsymbol{V}\cdot\nabla T_s - \nabla\cdot(\kappa\nabla T_s) + \alpha(T_s - T_f) - \dot{q}_s = 0 \tag{4}$$

In Eqs. (1)-(4), subscripts f and s denote the fluid and solid phases, respectively. ϵ is the pebble bed porosity, which is assumed time-independent, but shown within time derivatives to illustrate similarity to the Navier-Stokes equations. $\boldsymbol{V}$ is the intrinsic fluid velocity, P is the pressure, and $\boldsymbol{g}$ is the gravitational acceleration. k, ρ, C_p, E, and H are the thermal conductivity, density, isobaric specific heat, total energy, and total enthalpy. During the averaging process, several closure terms appear to represent momentum and energy transfer between the phases. W is the interphase drag coefficient, κ is the effective solid thermal conductivity, and α is the interphase heat transfer coefficient; these terms are available from experimental investigations of porous media. $\dot{q}$ is a generic heat source, which may represent fission heat in the fuel or gamma heating in the coolant. The effects of the viscous stress tensor on momentum are approximated with a distributed loss model via W, while viscous dissipation and pressure work are neglected in the fluid energy equation. Eqs. (1)-(4) are here referred to as the "compressible porous media" equations.

In addition to the compressible porous media equations, Pronghorn contains a second flow model that is here referred to as the "low-advection porous media" equations. For negligible momentum advection, the total derivative of momentum may be neglected in Eq. (2), giving a simpler momentum equation,

$$\epsilon\nabla P - \epsilon\rho_f \boldsymbol{g} + W\rho_f \boldsymbol{V} = 0\,. \tag{5}$$

Substituting Eq. (5) into Eq. (1) gives a pressure Poisson equation that is generally easier to solve with the Finite Element (FE) method than the advective Eq. (1),

$$\frac{\partial(\epsilon\rho_f)}{\partial t} + \nabla\cdot\left[\frac{\epsilon^2}{W}\left(-\nabla P + \rho_f \boldsymbol{g}\right)\right] = 0\,. \tag{6}$$

The low-advection porous media equations are therefore represented by Eqs. (6), (5), (3), and (4). A primitive form of Eq. (3) that is solved for temperature, rather than total energy, is also available. The full details on the derivation of the various flow models and the closure terms is available in the Pronghorn theory manual [1].

RESULTS

This describes validation efforts of the low-advection porous media equations and the non-conducting, non-porous equivalent of the compressible porous media model, with selected results.

Validation of the Low-Advection Model

In order to validate the expected thermal stability and heat removal characteristics of HTRs, a large experimental validation program, known as the SANA experiments, was conducted in Germany from 1994 to 1996 [2]. The SANA

facility consists of a cylindrical vessel containing about 9500 graphite pebbles, electrically heated by resistance heater elements at various locations within the bed and cooled by nitrogen, helium, or argon. Over 50 experiments were completed, but for validation purposes only six were simulated with Pronghorn [3]. This section briefly discusses simulation results obtained for helium and nitrogen coolants with a single centrally-located heater element at two power levels - 10 and 35 kW for helium, and 10 and 25 kW for nitrogen.

The azimuthally symmetric geometry is modeled using a 2-D cylindrical mesh; all insulation layers and thermocouples are neglected for simplicity. The heat flux from the central rod is assumed split in a $1-\epsilon$:ϵ ratio between the solid and the fluid, and a constant porosity is assumed throughout the bed. At the outer wall, it is assumed that the fluid transfers its heat first to the solid phase, and then the solid transfers its heat directly to the ambient via natural convection and radiation. For simplicity, no vessel wall is explicitly modeled. Zero normal velocity is imposed on all boundaries such that the experiment represents steady state LOFC decay heat removal. Details on the closure relationships used for W, κ, and α is available in the literature [3].

Correlations for helium density, viscosity, thermal conductivity, and a constant value for specific heat are obtained from the literature [3]. A generalized fluid properties module is under development in MOOSE, and to avoid duplicating those efforts, constant thermophysical properties are assumed for nitrogen viscosity, thermal conductivity, and specific heat, while the ideal gas law is used for density. Figs. 1 and 2 show the experimental thermocouple and Pronghorn simulation results for helium coolant at 10 and 35 kW, respectively, at three different elevations measured from the bottom of the vessel.

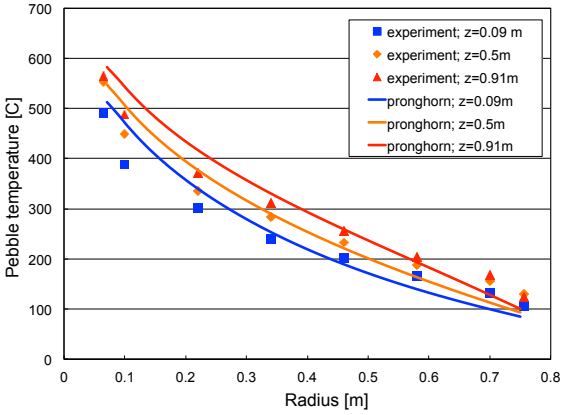

Fig. 1. Experimental and Pronghorn radial solid temperature at three different elevations for helium at 10 kW.

For these helium cases, temperatures tend to be overpredicted near the center of the bed, and underpredicted near the outer periphery. Reasonable temperature predictions are obtained in the bulk of the bed, with the largest errors occurring at lower power. Figs. 3 and 4 show the experimental thermocouple and Pronghorn simulation results for nitrogen coolant at 10 and 25 kW, respectively, at the same three elevations. At 600°C and 1 atm, the thermal conductivity of helium if about 5.5 times larger than that of nitrogen. Because nitrogen

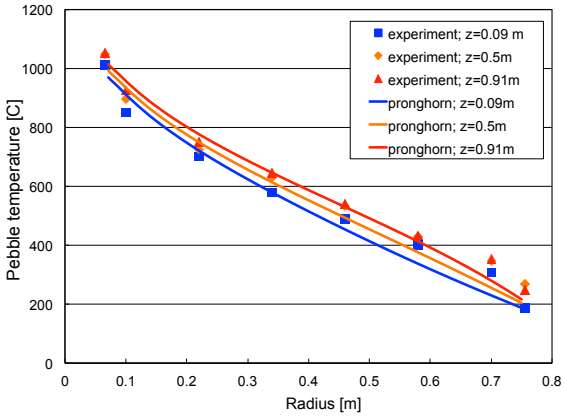

Fig. 2. Experimental and Pronghorn radial solid temperature at three different elevations for helium at 35 kW.

does not conduct heat as efficiently as helium, a larger portion of the heat transfer occurs by natural convection, producing much larger axial gradients in Figs. 3 and 4 than in Figs. 1 and 2.

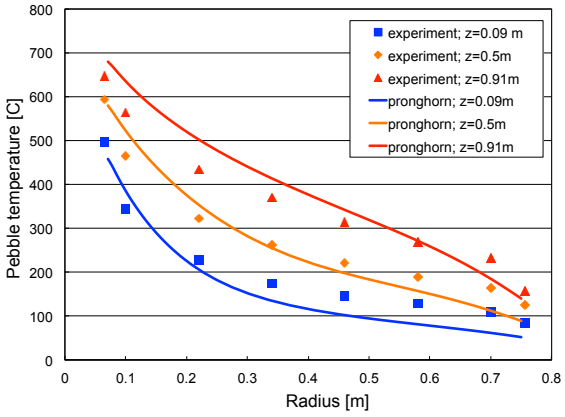

Fig. 3. Experimental and Pronghorn radial solid temperature at three different elevations for nitrogen at 10 kW.

In general, the Pronghorn simulation results for nitrogen are less accurate than those for helium. For all cases, errors on the bed peripheries can be partially attributed to the use of a constant porosity and simplifications made in the geometry representation and application of boundary conditions [3]. Larger errors near the edges of a porous media, especially near very localized heat sources, are to be expected simply due to the nature of the porous media assumption, which treats the packed bed as a continuum. Contrary to helium, the largest errors in the nitrogen cases occur in the bulk of the bed, where the porous media approximation is the "most valid." These errors are most likely caused by the use of constant material properties, aside from density, for nitrogen, especially since larger axial temperature gradients make the use of constant properties less accurate.

Generally, errors are highest at the lowest elevations of the bed, which may be attributed to the assumption of zero inlet velocity that was necessary due to a lack of inlet flowrate data in the benchmark specifications [2]. Another source of error is

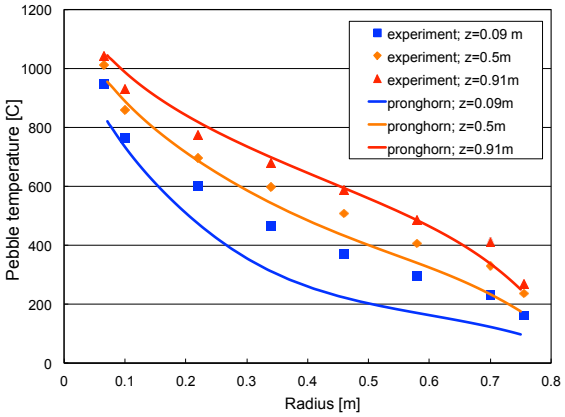

Fig. 4. Experimental and Pronghorn radial solid temperature at three different elevations for nitrogen at 25 kW.

the uncertainty in porous media closure relationships in general. The results were found to be very sensitive to the closure relationship selected for κ, with different correlations resulting in up to 75°C temperature differences in the bed center. In addition, low flowrates outside the regime of applicability of the closure relationship for α require the identification of additional closure relationships.

A brief code-to-code comparison shows that the results displayed in Figs. 1-4 are of similar accuracy to those obtained with comparable porous media codes. For example, errors for the 10 kW helium case are frequently on the order of 50-100°C, especially near the bed periphery [3]. This comparison of Pronghorn simulation results against the experimental data and comparable porous media codes demonstrate that within the limits of the porous media approximation, the low-advection model is capable of simulating LOFC conditions in gas-cooled HTRs.

Validation of the Compressible Euler Model

The field of compressible fluid dynamics is well-developed, and many classic problems have been formulated with either analytic, approximate, or experimental data to provide model validation. Significantly less validation data is available for the compressible porous Euler equations. For this reason, validation of the compressible porous media model in Eqs. (1)-(4) is deferred to later studies, and the validation discussed here focuses only on the validation of the non-porous media, non-conducting, equivalents of Eqs. (1)-(4) which are obtained by setting $\epsilon = 1$, $k_f = 0$, $W = 0$, and $\alpha = 0$. Eqs. (1)-(4) with these modifications are here referred to as the "compressible Euler" equations. It should be noted that Pronghorn can solve Eqs. (1)-(4) as-is, i.e. in porous form with all closure laws included, but validation of this model is deferred to future work. This permits the validation process of the compressible porous flow model in Pronghorn to proceed incrementally.

This section presents validation results for low Mach number flow of a compressible fluid over a circular cylinder. For uniform initial conditions and uniform inflow conditions, the Euler equations are physically equivalent to the potential flow equations, a simplification of the Euler equations for irrotational flow. For incompressible flow, an analytic solution to the potential flow equations exists for flow over a circular cylinder. Therefore, validation of the compressible Euler equations in Pronghorn with the analytic incompressible potential flow solution is possible for low Mach numbers where compressibility effects are small.

The analytic solution for incompressible potential flow around a circular cylinder can be obtained as a superposition of the solutions for uniform flow and a doublet [4]. For incompressible uniform inflow of a fluid at velocity U over a cylinder of radius R centered at $x = 0$ and $y = 0$, the velocity components are given as

$$V_x = U\left[1 - \frac{R^2(x^2 - y^2)}{(x^2 + y^2)^2}\right], \tag{7}$$

$$V_y = -2UR^2\frac{xy}{(x^2 + y^2)^2}. \tag{8}$$

Compressible Euler simulations have been performed in Pronghorn for inlet Mach numbers ranging from 0.1 to 0.5 for air at atmospheric pressure and temperature, the flow becoming transonic for an inlet Mach number of 0.5. For validation purposes, only results at an inlet Mach number of 0.1 are shown here, for which the errors in the velocity relative to Eqs. (7) and (8) should be small, despite comparison being made between a compressible rotational model and an incompressible irrotational analytical solution. Figs. 5 and 6 shows the velocity streamlines and contour, colored with velocity magnitude. Flow is from left to right.

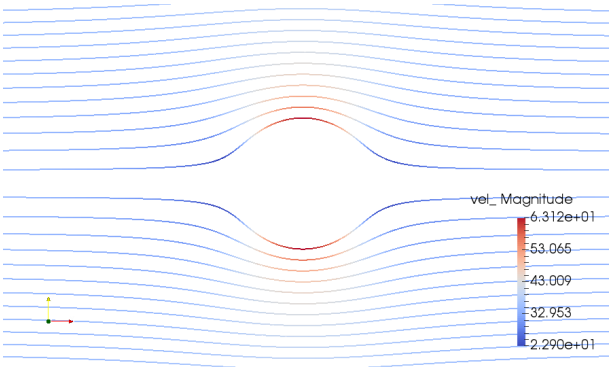

Fig. 5. Velocity streamlines, colored with velocity, for an inlet Mach number of 0.1

Qualitatively, these results agree very well with the analytic solution [4]. Fig. 7 shows the elementwise relative L-2 norm of the velocity error, taking Eqs. (7) and (8) as the true solution. Only a subset of the computational domain is shown; the relative error ranges from 1.89×10^{-4} to a maximum of 2.35×10^{-2}. Less than 3% peak error, considering the comparison of a fully compressible rotational model to an incompressible and irrotational analytic solution, validates the compressible Euler model in Pronghorn. Mesh refinement studies and additional error metrics such as the pressure coefficient along the cylinder surface, not shown here, further support this conclusion.

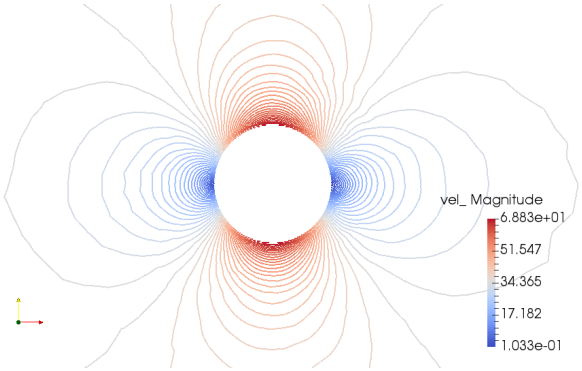

Fig. 6. Velocity contours, colored with velocity, for an inlet Mach number of 0.1

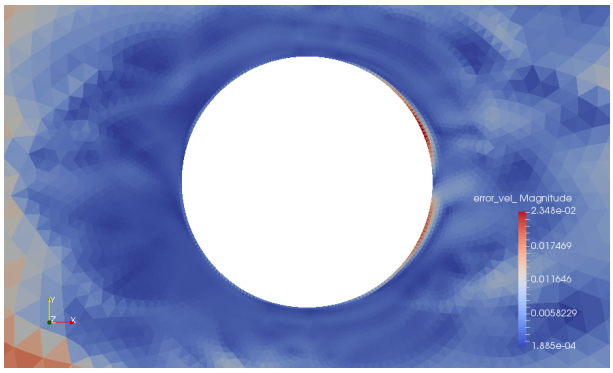

Fig. 7. Elementwise relative L-2 norm of the velocity error for an inlet Mach number of 0.1.

For Mach numbers greater than about 0.5, the flow becomes transonic, and a comparison against the incompressible potential flow solution would not be useful due to the very different physics involved. For the purposes of demonstrating the capabilities of the newly-added compressible Euler model, Fig. 8 shows the velocity vector field, background colored with velocity, for an inlet Mach number of 0.5 for air at atmospheric pressure and temperature. At the time shown in Fig. 8, the Mach number ranges from 2.33×10^{-3} to 2.09. Pronghorn's ability to capture a shock at $\theta \approx \pi/2$ on the cylinder surface and vortices behind the cylinder demonstrate the use of Pronghorn as a general compressible Euler solver, in addition to its porous media capabilities.

CONCLUSIONS

Porous media models of pebble bed reactors have runtimes about 1% or less than those of detailed CFD models and employ much simpler meshes. At the expense of approximating the local flow and heat transfer effects, medium-fidelity simulations can be performed to accelerate the design and analysis cycle for pebble bed HTRs. This paper has described two flow models available in Pronghorn - one appropriate to low-momentum-advection flows typical of LOFC conditions and another appropriate to general compressible flow. Validation of the porous low-advection model with the SANA experiments and of the nonporous compressible Euler model with

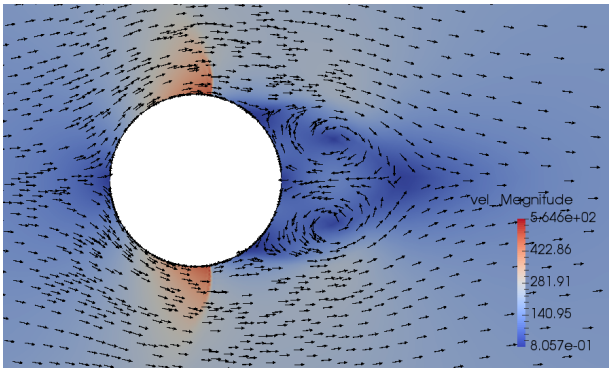

Fig. 8. Velocity vector field, colored with velocity, for an inlet Mach number of 0.5.

low Mach number flow over a cylinder has been presented. Ongoing work focuses on improving the SANA simulation results via model sophistication and extending the compressible Euler model validation to include porous media and conditions typical of gas-cooled reactors.

The development of Pronghorn is motivated by the desire to permit 1) an arbitrary equation of state appropriate for both gas- and liquid-cooled HTRs, 2) simulation on unstructured meshes, 3) the use of modern software practices, and 4) relatively easy coupling to other MOOSE framework codes to facilitate interesting multiphysics simulations incorporating nuclear fuels, systems-level thermal-hydraulics, and many other applications. This paper has presented validation efforts in support of this mission.

ACKNOWLEDGMENTS

This material is based upon work supported by a Department of Energy Nuclear Energy University Programs Graduate Fellowship.

REFERENCES

1. A. J. NOVAK, L. ZOU, J. W. PETERSON, D. ANDRS, J. KELLY, R. N. SLAYBAUGH, R. C. MARTINEAU, and H. D. GOUGAR, "Pronghorn Theory Manual," Tech. Rep. INL/EXT-18-44453, Idaho National Laboratory (2018).
2. B. STOCKER and H. NIEBEN, "Data Sets of the SANA Experiment 1994–1996," Tech. rep., Forschungszentrum Julich (1996).
3. A. J. NOVAK, L. ZOU, J. W. PETERSON, R. C. MARTINEAU, and R. N. SLAYBAUGH, "Pronghorn: A Porous Media Thermal-Hydraulics Core Simulator and its Validation with the SANA Experiments," in "Proceedings of ICAPP," (2018).
4. C. HIRSCH, *Numerical Computation of Internal and External Flows*, Butterworth-Heinemann (2007).